Experimental verification of isotropic and polarization properties of high permittivity-based metamaterial

Fuli Zhang,[1,2] Qian Zhao,[3] Lei Kang,[4] Ji Zhou,[4] and Didier Lippens[1,*]

[1]*Institut d'Electronique de Microélectronique et de Nanotechnologie, CNRS 8520, Université des Sciences et Technologies de Lille, 59652 Villeneuve d'Ascq Cedex, France*

[2]*Department of Applied Physics, Northwestern Polytechnical University, Xi'an 710072, People's Republic of China*

[3]*State Key Laboratory of Tribology, Department of Precision Instruments and Mechanology, Tsinghua University, Beijing 100084, People's Republic of China*

[4]*State Key Laboratory of New Ceramics and Fine Processing, Department of Materials Science and Engineering, Tsinghua University, Beijing 100084, People's Republic of China*

(Received 14 August 2009; published 30 November 2009)

We report on the experimental verification of isotropy and polarization properties of high-permittivity metamaterial composed of cubic ferroelectric resonators. Barium strontium titanate (BST) with permittivity as high as 850 is used as ferroelectrics material so that the metamaterial condition is fulfilled. The isotropy was investigated via the scattering of an electromagnetic wave under tilted incidence. From the experimental data, we observed that the magnetic resonance, at 8.6 GHz for a millimeter cube size, is independent of the incidence angle for the TM and TE polarizations. For the latter, however, an extra dip in the transmittance at higher frequency (10.7 GHz for a period of 1.2 mm), not evident under normal incidence, is found. By comparing the full wave simulations of microstructured and homogenous metamaterial slabs it is shown that the electromagnetic response is independent of the underlying structuring technique. On this basis, we verified that this extra dip, theoretically predicted by [Koschny *et al.*, Phys. Rev. B **71**, 121103(R) (2005)] for a three-dimensional split ring resonator technology, results from the permeability dispersion characteristics of BST cubes, with zero transmittance at the magnetic plasma frequency.

DOI: 10.1103/PhysRevB.80.195119 PACS number(s): 42.25.Bs, 78.20.Ci, 77.84.−s, 77.90.+k

I. INTRODUCTION

Since the experimental demonstration of the left handedness of split ring resonator (SRR) and wire arrays with simultaneous negative values of permittivity and permeability,[1–4] the realization of an isotropic metamaterial, with electromagnetic properties independent of wave polarization, has attracted much attention, with notably the prospect of a perfect lens.[5] Shelby *et al.*[6] have investigated a two-dimensional isotropic left-handed metamaterial (LHM) by arranging SRR/wire in an orthogonal lattice. Koschny *et al.*[7] numerically studied the transmission property of an isotropic LHM composed of a multigap symmetric SRR and crossing wires. However, the intrinsically anisotropic properties of SRR, due to its planar configuration, have restricted greatly the practical realization of these three-dimensional isotropic metamaterials. On the other hand, the Ohmic losses in metallic inclusions also limit the suitability of this technology at very high frequency notably at Terahertz frequencies.

An alternative for the fabrication of an isotropic metamaterial is to employ very high dielectric constant materials on the basis of the so-called Mie resonance. In fact, several theoretical analyses showed that high dielectric spheres[8–10] or cylinder[11] can create single or double negative media. Popa and Cummer[12] have shown that a dielectric magnetic resonator has the significant advantages of low loss and simply geometry in comparison with a typical SRR. A recent experimental demonstration of negative refraction, in a wedge-type prototype composed of dielectric cylinders, was published in Ref. 13. Zhao *et al.*[14] experimentally studied a negative permeability metamaterial based on $Ba_{0.5}Sr_{0.5}TiO_3$ (BST) cubes which was subsequently associated with wire array to provide a passband with double negative effective parameters. Despites these works paved the way for full dielectric approaches to realize metamaterial, an analysis of their isotropy and polarization properties is still lacking.

In the present paper, we report on an experimental study of the isotropy and polarization conditions of an artificial magnetic metamaterial fabricated with arrayed high permittivity ($\varepsilon r \sim 850$) ferroelectric BST cubes. Scattering parameter measurements were conducted under normal and tilted incidences at microwave for millimeter-sized cubes. The analysis of the complex transmittance experiments was carried out by full-wave finite-element calculation notably by comparing the results of a microstructured material and of its homogenous counterpart. The isotropy of the electromagnetic characteristics of the magnetic resonant mode was verified experimentally whatever the polarization condition, showing a weak impact of the corner effect of cubes. Surprisingly for the transverse electric (TE) polarization and for tilted incidences, an extra dip in the transmittance was found. The analysis of this extra feature reveals that it results from the same effect for three-dimensional (3D) SRR arrays as predicted theoretically in Ref. 7, i.e., a zero transmittance occurs at the magnetic plasma frequency. Basically, this effect results from the finite dimension of the slab in the propagation direction and it disappears under normal incidence. Therefore, the frequency dependence on the dispersion characteristic of constitutive materials gives a means to decouple the polarization-independent ground magnetic response from the polarization-sensitive one.

II. NUMERICAL ANALYSIS

For the practical realization of the BST ferroelectric inclusion fabricated by casting and dicing techniques,[14] a cubic cell was chosen rather than a spherical one. The barium concentration which determines the Curie temperature was 50% ($Ba_{0.5}Sr_{0.5}TiO_3$). The ferroelectric ceramic permittivity, measured by a conventional resonance perturbation method, was close to one thousand at room temperature. The BST cubes were arrayed, with a pitch of 1.25 mm, by using a Teflon host substrate whose relative permittivity is low (ε_r=2.1). Under this condition with a high difference between the permittivities of BST cubes and host substrate, most of the electromagnetic is confined in the dielectric cubes. This is a necessary condition to operate in the long-wavelength regime so that the metamaterial condition is satisfied. In other words, the resonance gap is at much lower frequencies than the Bragg one. The lowest order resonant mode frequency of a cubic dielectric resonator can be expressed by[15,16]

$$f = \frac{c_0}{\sqrt{2}\sqrt{\varepsilon_r \mu_r} l}, \tag{1}$$

where c_0 is light velocity in vacuum, ε_r and μ_r are the relative permittivity and permeability of dielectric cubes, and l is the side length of the cube. In the experiment, we chose a type of BST with a relative permittivity of $850+25i$, which is doped by 5 wt % MgO.[17] A value of the permittivity of 850 was measured at 2.4 GHz. We kept this value constant at the frequency of interest around 9 GHz on the basis of relaxation mechanisms which take place at Terahertz frequencies.[18] The side length of the cube l after dicing is 0.9 mm. Thus, the first-order resonant frequency is estimated around 8.1 GHz from Eq. (1).

For the design and interpretation of the experimental data we used the finite-element simulation code commercialized by Ansoft, high-frequency structure simulator (HFSS). Figure 1 illustrates (a) the condition of simulation of a basic cell and (b) of its homogeneous equivalent. As shown in Fig. 1, the incidence of electromagnetic plane was characterized by two angles: the incidence angle θ between the wave vector **k** and surface normal to the slab and the angle ϕ between the projection of **k** and a reference side of the sample. For the calculations of the transmittance complex amplitudes (scattering parameter S_{21}), for any incidence angle, we used the so-called Floquet port and master slave boundaries available in version 11 of the code.

The periodicity of the basic unit cell (a=1.25 mm) is approximately 25 times smaller than the incident wavelength in free space at the frequencies of interest. This allows us to consider the dielectric inhomogeneous structure as a homogenous one by using effective medium theory. To this aim, we computed the scattering parameters of a basic cell under a normal incidence, according to the boundary conditions outlined above, when θ and ϕ=0. The scattering parameters were then converted into effective parameters by using an inverse algorithm.[19–21]

Figure 2 shows the retrieved effective $\mu(\omega)$ and $\varepsilon(\omega)$ for a ferroelectrics cubic array whose dimensions are listed in the caption of Fig. 1. The effective permeability $\mu(\omega)$ for the high-permittivity metamaterial exhibits a Lorentz-type dispersion characteristics with a resonance frequency around 9.0 GHz. The effective permeability is negative up to the magnetic plasma frequency, ω_{mp}, at 10.6 GHz. From the displacement currents map as shown in Fig. 1(c), it can be verified that the artificial magnetism found here results from a resonant magnetic dipole within the corresponding current loop.[22] Therefore, this effect is quite comparable to the one pointed out in SRR by replacing conductive current by dis-

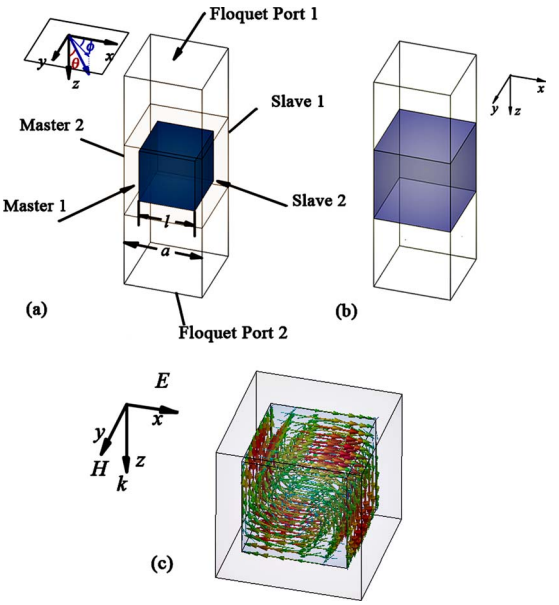

FIG. 1. (Color online) (a) Model of a full dielectric metamaterial consisting of BST cubes under oblique incidence. The geometry dimensions of the elementary cell are: l=0.9 and a=1.25 mm. Teflon (ε=2.1 tan δ=0.001) was chosen to host the BST dielectric cubes. Floquet ports and master and slave periodic boundaries (HFSS code) are used. (b) Schematic of a model for a homogenous dielectric metamaterial. The dielectric and magnetic material properties are defined by using the effective permittivity and permeability depicted in Fig. 2. (c) Zoom view of circular displacement currents induced by an external magnetic field around the magnetic-resonance frequency, ω_m=9.0 GHz.

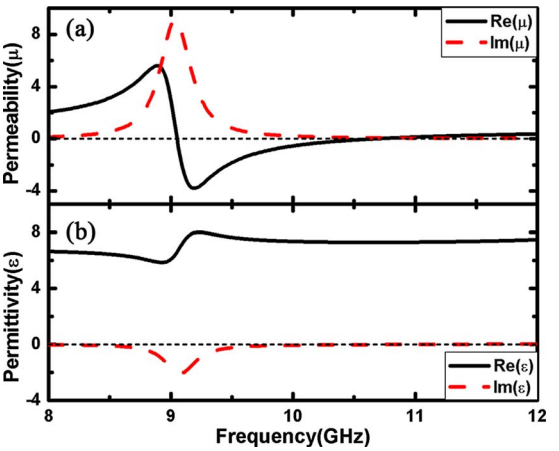

FIG. 2. (Color online) (a) Effective permeability and (b) permittivity of the dielectric metamaterial under normal incidence.

placement current. The main and important differences are, however, that the very strict polarization condition (H direction normal to the SRR plane) and symmetry configuration (multigap scheme), which have to be satisfied for the planar SRR structures, are here relaxed by the simple use of a dielectric cube. In addition it is worth mentioning that contrary to the split ring resonator scheme where a single or multislot configuration was introduced, the basic cell was made of a bulk ceramic cube and hence without any slot or trench explaining the resonance pattern displayed in Fig. 1(c).

Compared to the magnetic-resonance frequency predicted by Eq. (1), there is a discrepancy around 10%. From Fig. 1(c), it can be shown that circular-type currents quite similar to those of infinite cylindrical dielectric rods[11] may break out the square-shape constraints.[13] This can lead to smaller apparent confinement condition via ε_r and l and hence to higher resonant frequency. In addition, this is a first clue that the square shape should have a weak impact on isotropy properties. The frequency dependence of the effective permittivity is almost constant except an antiresonance feature at 9.0 GHz with an unphysical negative value of the imaginary part as a result of periodicity effects.[23] Let us note that a physical permittivity response could be obtained at higher frequencies therefore for a second-order mode.[9,14]

In order to assess the sensitivity of a metamaterial slab to an arbitrary incidence angle and polarization, two fundamental operating modes were defined, TE and TM, respectively. They correspond to a polarization direction either of the electric field or the magnetic field parallel to the dielectric slab, with various θ angles (see inset of Fig. 1). Figure 3 shows the calculated transmission spectra for a one-row slab for various incidence angles between 0° and 60° and for both polarizations TE and TM. For the normal incidence, a dip occurs at 9.1 GHz, corresponding to the magnetic resonance as illustrated in Fig. 1(c). When the incidence beam **k** vector is misaligned with respect to the surface normal, the magnetic-resonance dip position and magnitude is practically unchanged at least up to 45° for the amplitude. This result reveals an independence of the ground magnetic resonant mode on incidence direction and on polarization. The overall increase in the insertion loss at large angle incidence is explained by the use of one-row slab with an increasing involvement of neighbor cubes. Despite the square-shaped dielectric structure, the scattering parameter S_{21} was found independent of ϕ (not shown here) whatever the polarization and incidence angle. This is in agreement with the numerical results of SRR cubic lattice simulations reported in Ref. 7. An important difference exists between both polarizations with the appearance of a transmission dip, here around 10.7 GHz, for off-normal axis incidences.

In order to show that this extra zero of transmission is quite general and is independent of the structuring technique, we simulated the transmission spectra for a homogenous slab characterized by using the effective permeability and permittivity reported in Fig. 2. The transmission results of homogenous and microstructured cases were plotted by a solid line and hollow circles in Fig. 3, respectively. A very good agreement was obtained showing the possibility to treat the microstructured array as a homogenous one. More importantly, an extra dip is also apparent around 10.7 GHz giving some evidence that this extra transmission feature results from the intrinsic dispersion of the effective parameters rather than structuring. The slight discrepancy (blueshift of the characteristic frequency of the second dip for the microstructure) stems from the invariance of the permeability dispersion characteristic for a homogenous layer contrary to a composite device.[7]

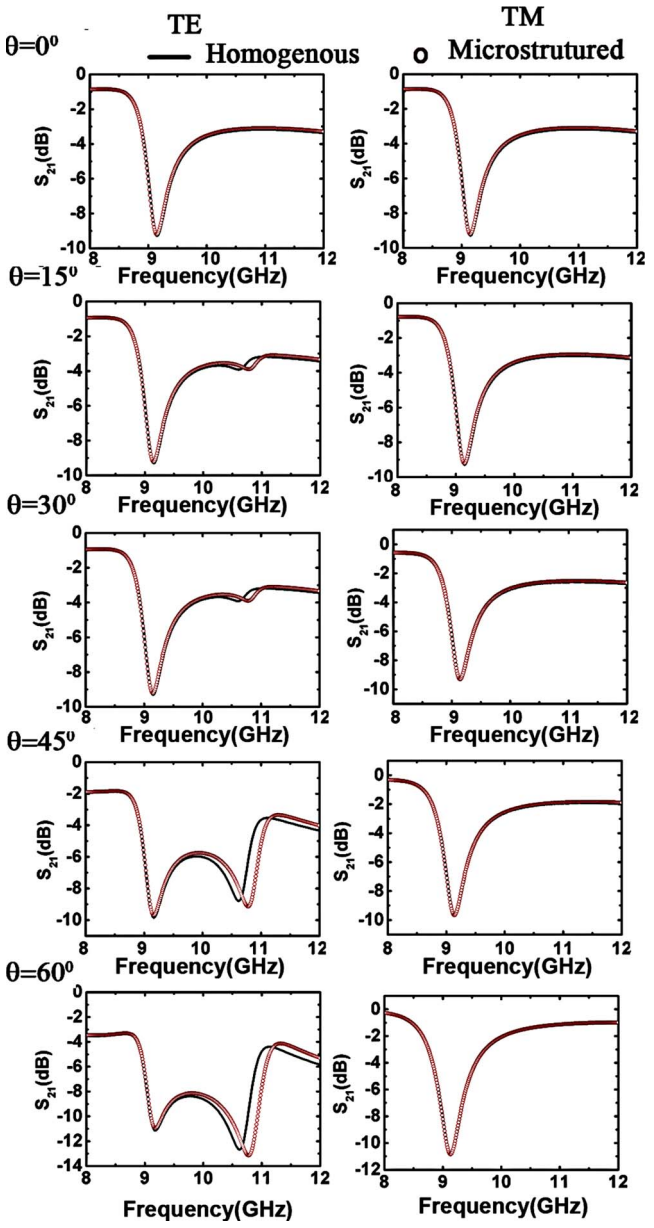

FIG. 3. (Color online) Transmission spectra for a single layer of dielectric negative permeability metamaterial under various incidence angles θ (ϕ=45°) and modes (TE and TM).

A similar dip in the transmittance was already predicted theoretically in the literature by numerically studying the frequency response of negative magnetic artificial media. It was thus shown that this phenomenon is due to a zero in the permeability dispersion $\mu(\omega)$ around magnetic plasma frequency.[7] Indeed for a homogenous slab with permittivity ε and permeability μ, the dispersion relation is

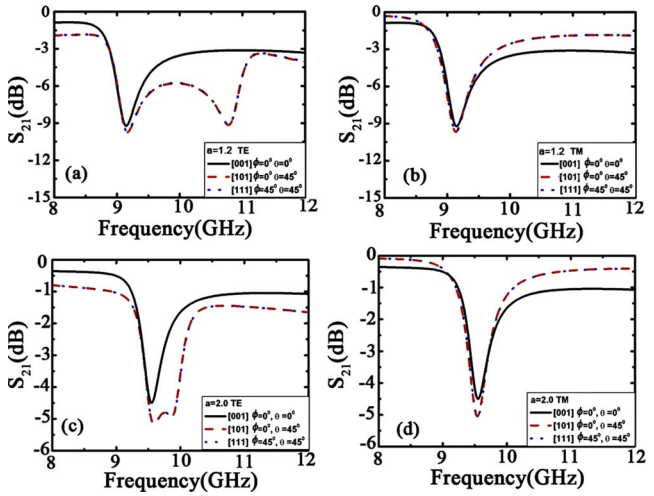

FIG. 4. (Color online) Transmission spectra for a layer of dielectric negative permeability metamaterial along three principal directions (x, y, and z) of a cube cell by considering TE and TM (b) modes with lattice [(a), (b)] $a=1.25$ and [(c), (d)] $a=2.0$ mm, respectively.

$$k_{\perp}^2 + k_{\parallel}^2 = k_0^2 \varepsilon \mu, \tag{2}$$

where k_0 is the wave vector in vacuum, $k_{\perp}$ and $k_{\parallel}$ are the wave-vector components perpendicular and parallel to the surface of the slab, respectively. The analytical transmission amplitude T can be expressed[7]

$$T^{-1} = \cos k_{\perp} d - (i/2)(\zeta + 1/\zeta)\sin k_{\perp} d, \tag{3}$$

where d is the slab thickness, and $\zeta = \mu k / k_{\perp}$ for TE mode and $\zeta = \varepsilon k / k_{\perp}$ for TM mode respectively. When $\mu(\omega)$ for TE mode or $\varepsilon(\omega)$ for TM equals zero, the inverse of the transmission T^{-1} diverges by the prefactor of the second term, yielding a vanishing transmission for off-normal incidence. In case of normal incidence the divergence is compensated by the vanishing term $k_{\perp}^2 = k_0^2 \varepsilon \mu$. A verification of this interpretation can be achieved by checking that the extra dip in Fig. 3 in the TE transmission spectra is at the magnetic plasma frequency, ω_{mp}, where the dielectric resonator exhibits zero permeability (Fig. 2).

Before considering the experimental verification of the dispersion effects pointed out above, it seems interesting to study the lattice conditions of insensitivity to incidence and polarization. Toward this goal, Fig. 4 compares the transmission spectra along three principal axes of the cube, namely, [100] ($\theta=0$, $\phi=0$), [101] ($\theta=0$, $\phi=45°$), and [111] ($\theta=45°$ $\phi=45°$) for two values of lattice constants, 1.25 and 2.00 mm, respectively. By comparing the transmission spectra it can be noticed that the two dips are much closer for the TE polarization when the lattice is increased 2.00 mm, thus starting the formation of a gap at increasing incidence angle. Importantly, for each lattice, the magnetic-resonance frequency of dielectric resonator is independent of the incidence angle and polarization.

According to the aforementioned interpretation, the frequency corresponding to the second zero transmission is related to the magnetic plasma frequency, ω_{mp}, that depends on the filling factor and on the resonance frequency ω_m by the relation.[3,12]

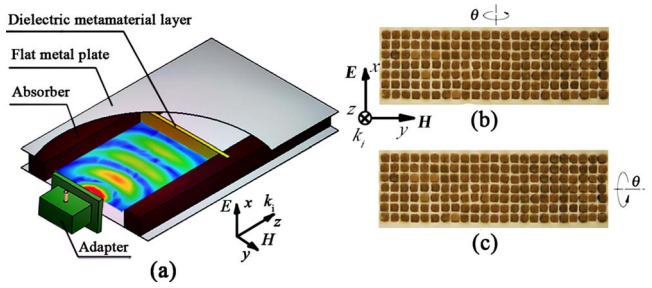

FIG. 5. (Color online) (a) Schematic view of experimental setup. The front view of a dielectric metamaterial sample consisting of BST cubes in a square lattice. The single layer is rotated around the x and y axes to measure the transmittance for (b) TE and (c) TM modes with various incidence angles θ ($\phi=0°$), respectively.

$$\omega_{mp} = \frac{1}{\sqrt{1-F}}\omega_m, \tag{4}$$

where $F = \frac{S}{a^2}$ is the area filling factor of the magnetic resonator. On this basis, it is expected that the second dip in the transmission spectra of TE mode changes with the periodicity. By decreasing the filling factor via a change in the periodicity (2.00 mm rather than 1.25 mm) the second dip is dramatically decreases to 9.86 GHz for TE mode so that a bandgap appears. This further confirms our assumption that the second dip is arising from the vanishing permeability at magnetic plasma frequency and shows the importance of the lattice constant.

III. EXPERIMENTAL RESULTS

As shown by the simulations results stated above, the frequency positions of the first and second dips for TE mode will be closer when the elementary cell periodicity becomes larger. This may somewhat bring some difficulties in distinguishing the two dips for an experimental assessment. As a consequence, we chose a periodicity (1.25 mm) exceeding slightly the cube size (0.9 mm) for experiment which was carried out with a one row-layer prototype as depicted in Fig. 5. Ideally, transmission measurements should be performed in free space as performed recently for bulk array of SRR-type metamaterials.[24,25] In the present case of millimeter-sized high-permittivity cubes operating at centimeter wavelengths, this would require that the lateral dimensions of the sample under test exceed the wavelength of interest and consequently more than several thousand dielectric cubes which were not affordable owing to the fabrication techniques we used. As a consequence, we performed the measurement by using a parallel plate setup which has been extensively used in metamaterial characterizations.[2,6,26] A schematic of the set up is shown in Fig. 5(a). A single layer of dielectric metamaterial, composed of BST cubes embedded into a Teflon template, was clad by two absorbers on each side in order to eliminate spurious reflections. The incident beam is generated by the flange of a hollow waveguide (in practice a

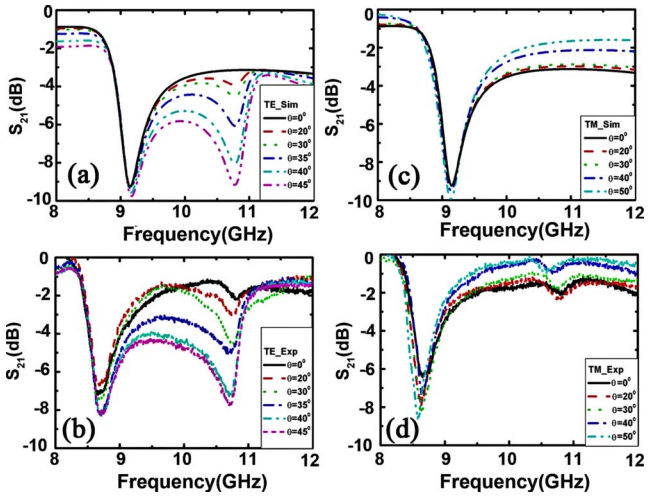

FIG. 6. (Color online) The simulated [(a), (c)] and experimental [(b), (d)] oblique transmission spectra for the single layer of dielectric metamaterial with TE and TM modes.

coaxial-waveguide adapter) rather than a horn. The spatial extension of the wave was controlled by absorbing layers as illustrated in Fig. 5(a). From the simulation results reported above, it was found that the scattering amplitude of the cubic dielectric resonator is independent of the angle ϕ between the incidence plane and cube edge. This makes the experimental measurement more simplified, and hence only the case $\phi=0°$ was considered. To perform measurements under oblique incidence, we rotated the metamaterial layer along the x (the direction of **E** field) and y axes (the direction of **H** field) for the transmission spectra of TE and TM modes, respectively, as shown in Figs. 5(b) and 5(c). The complex transmission data were recorded by using a HP8720 ES Vectorial Network Analyzer.

Figure 6 shows the experimental and calculated transmission spectra recorded between 8.0 and 12.0 GHz. For a normal incidence the dielectric metamaterial shows a transmission dip at 8.6 GHz, and thus with a slight discrepancy with respect to the simulated results. Afterwards, it was checked that the periodicity of the template fabricated by conventional micromachining technique exhibits a slightly smaller periodicity (closer to 1.1 mm) explaining why the resonant frequency is shifted to a lower frequency by proximity effects. In addition, some dispersion on the cube size was found with, however, a nominal value close to 0.9 mm. An unexpected minor dip occurs at 10.7 GHz, not found in the simulations for normal incidence. From the phase front illustrated in the schematic of the experimental setup, it can be noted a strict normal incidence of a plane wave is solely preserved in the middle region of the channel. In contrast, slightly tilted incidences of the electromagnetic waves cannot be avoided in the side areas. This explains why a slight dip appears at the magnetic plasma frequency under normal incidence with an imperfect cancellation of μ by $k_\perp$ [Eq. (3)].

When the metamaterial layer is rotated along the x axis, the electric field of the incidence beam is always parallel to the layer surface, equaling to the oblique incidence of the TE mode. As seen in Fig. 6(b), the second dip becomes more and more visible and its strength increases upon the tilted angle θ, becoming comparable to that of the first dip when $\theta=45°$. In contrast, the minor extra dip also shown for the TM polarization is unchanged for the measurement, further confirming the imperfection of the plane-wave excitation. On the basis of an overall good agreement with the calculations, a relative insensitivity of the first rejection at the magnetic-resonance frequency is here pointed out for both TE and TM modes.

To our knowledge, the effect of polarization on magnetic single negative media was predicted theoretically for a SRR technology but not experimentally assessed.

Compared to the SRR approach whose fabrication for an isotropic metamaterial is very challenging, the full dielectric approach has the advantage of a simpler geometry and no requiring a patterning stage. It is also worth mentioning that the achievement of a magnetic Mie resonance does not require an additional structuring stage such as a split which is commonly used starting from a closed ring in a metal dielectric technology. The latter thus requires balancing the anisotropy induced by the slot by patterning, for instance, Omega-type metal inclusion in a back-to-back configuration.[27] On the other hand, we learnt that the use of cubic inclusions instead of spherical ones as proposed[8–10] in previous works is not a handicap with respect the isotropic properties greatly facilitating the fabrication process.

IV. CONCLUSION

In this paper, an isotropic magnetic metamaterial composed of cubic BST resonators was proposed. The condition of high permittivity used here with very high values of permittivity was imperative to satisfy the long-wavelength regime. The isotropic properties of this dielectric metamaterial were investigated theoretically and experimentally via oblique incidence conditions for TE and TM polarizations of a single layer. In addition to the ground magnetic resonance dip which was found practically insensitive to incidence and polarization, an extra second dip, which only occurs for the oblique incidence of TE mode, was evidenced numerically and experimentally. It was shown that this extra response, shown here for a full dielectric approach, is similar to the one pointed out theoretically for a 3D SRR technology.[7] This effect, occurring for off-normal incidence, results from the dispersion of the effective permeability with a zero value at the magnetic plasma frequency. This result was further confirmed by varying the periodicity of the structure, and hence the filling factor, giving a practical means to decouple magnetic resonant and plasma frequencies.

ACKNOWLEDGMENTS

This work was carried out in the framework of a Delegation Générale à l'Armement Contract.

*Author to whom correspondence should be addressed; didier.lippens@iemn.univ-lille1.fr

[1] V. G. Veselago, Sov. Phys. Usp. **10**, 509 (1968).
[2] D. R. Smith, W. J. Padilla, D. C. Vier, S. C. Nemat-Nasser, and S. Schultz, Phys. Rev. Lett. **84**, 4184 (2000).
[3] J. B. Pendry, A. J. Holden, D. J. Ribbins, and W. J. Stewart, IEEE Trans. Microwave Theory Tech. **47**, 2075 (1999).
[4] J. B. Pendry, A. J. Holden, W. J. Stewart, and I. Youngs, Phys. Rev. Lett. **76**, 4773 (1996).
[5] J. B. Pendry, Phys. Rev. Lett. **85**, 3966 (2000).
[6] R. A. Shelby, D. R. Smith, S. C. Nemat-Nasser, and S. Schultz, Appl. Phys. Lett. **78**, 489 (2001).
[7] Th. Koschny, L. Zhang, and C. M. Soukoulis, Phys. Rev. B **71**, 121103(R) (2005).
[8] L. Lewin, Proc. Inst. Electr. Eng. **94**, 65 (1947).
[9] C. H. Holloway, E. F. Kuester, J. Baker-Jarvis, and P. Kabos, IEEE Trans. Antennas Propag. **51**, 2596 (2003).
[10] M. S. Wheeler, J. S. Aitchison, and M. Mojahedi, Phys. Rev. B **72**, 193103 (2005).
[11] S. O'Brien and J. B. Pendry, J. Phys.: Condens. Matter **14**, 4035 (2002).
[12] B.-I. Popa and S. A. Cummer, Phys. Rev. Lett. **100**, 207401 (2008).
[13] L. Peng, L. Ran, H. Chen, H. Zhang, J. A. Kong, and T. M. Grzegorczyk, Phys. Rev. Lett. **98**, 157403 (2007).
[14] Q. Zhao, L. Kang, B. Du, H. Zhao, Q. Xie, X. Huang, B. Li, J. Zhou, and L. Li, Phys. Rev. Lett. **101**, 027402 (2008).
[15] D. K. Cheng, *Field and Wave Electromagnetics*, 2nd ed. (Addison-Wesley, New York, 1989).
[16] J. Kim and A. Gopinath, Phys. Rev. B **76**, 115126 (2007).
[17] Q. Zhao, B. Du, L. Kang, H. Zhao, Q. Xie, B. Li, X. Zhang, J. Zhou, L. Li, and Y. Meng, Appl. Phys. Lett. **92**, 051106 (2008).
[18] G. Houzet, L. Burgnies, G. Velu, J.-C. Carru, and D. Lippens, Appl. Phys. Lett. **93**, 053507 (2008).
[19] D. R. Smith, S. Schultz, P. Markoš, and C. M. Soukoulis, Phys. Rev. B **65**, 195104 (2002).
[20] X. Chen, T. M. Grzegorczyk, B.-I. Wu, J. Pacheco, and J. A. Kong, Phys. Rev. E **70**, 016608 (2004).
[21] C. Croënne, N. Fabre, D. P. Gaillot, O. Vanbésien, and D. Lippens, Phys. Rev. B **77**, 125333 (2008).
[22] D. Gaillot, C. Croënne, F. Zhang, and D. Lippens, New J. Phys. **10**, 115039 (2008).
[23] Th. Koschny, P. Markoš, E. N. Economou, D. R. Smith, D. C. Vier, and C. M. Soukoulis, Phys. Rev. B **71**, 245105 (2005).
[24] F. Zhang, D. P. Gaillot, C. Croënne, E. Lheurette, X. Mélique, and D. Lippens, Appl. Phys. Lett. **93**, 083104 (2008).
[25] K. B. Alici and E. Ozbay, Opt. Lett. **34**, 2294 (2009).
[26] F. Zhang, G. Houzet, E. Lheurette, D. Lippens, M. Chaubet, and X. Zhao, J. Appl. Phys. **103**, 084312 (2008).
[27] C. R. Simovski and S. L. He, Phys. Lett. A **311**, 254 (2003).